Modelling and Design Performance Analysis of the SRM Drive System

Abdelhamid Boucetta, M.L. Bendaas and O. Fadli
Faculty of Sciences Engineering, University of Batna,
Rue Chahid Med Elhadi Boukhlouf, 05000 Batna, Algeria

Abstract: A dynamic simulation of the drive system enables verification of the analytical designs and ability of the motor drive system to match the load torque over its entire speed range both in its steady state and during transients. With such verification, time and cost of product development are minimized by avoiding a trial-and-error approach to prototype construction that may lead to repetitive testing and redesign until specifications are met. Such a trial-and-error process in design is very costly and time consuming. Simulation of the drive system requires models for the SRM drive subsystems and their interconnections. The simulation procedure is also illustrated with many cases of SRM operation. This study presents a procedure for designing an SRM, selecting a suitable converter topology to drive it and designing a current controller, torque-smoothing controller and speed controller for the purpose of getting a high SRM drive performance.

Key words: Synchronous Reluctance Motors (SRM), speed and torque position controller, drive system

INTRODUCTION

The SRM drive system simulation is much more complex than ac and dc motor drives because its operational region is mostly nonlinear. The nonlinearity is introduced by the following three factors:

- The nonlinear B-H characteristics of the magnetic material.
- The dependence of phase flux linkages on both the rotor position and current magnitude, in other machines, it is dependent only on the current magnitude as the rotor position dependence is eliminated artificially with trigonometric transformations not feasible with an SRM.
- The single source of excitation. Meanwhile, in separately excited dc machines and synchronous machines having two sources of excitation, one for its field and the other to the armature. In these, the torque is proportional to the product of the armature and field currents. The system is made linear by keeping the magnetization (field) current constant, thus making the torque-producing part of the (armature) current a variable to provide a variable air gap torque as in the case of dc and ac machines. The implication of the excitation source being single is that the machine's torque is proportional to the square of the excitation current, among other things, resulting in a nonlinear system through the coupling of the air gap torque to the load through the

mechanical system. The inability to separate the excitation current into a magnetizing or flux-producing part and a torque-producing part makes it difficult to obtain a high-performance control in the SRM drives.

This study presents a procedure for designing an SRM, selecting a suitable converter topology to drive it and designing a current controller, torque-smoothing controller and speed controller. Simulation of the drive system requires models for the SRM drive subsystems and their interconnections. The simulation procedure is also illustrated with many cases of SRM operation.

TORQUE PRODUCTION

The torque production for motoring and regeneration is also shown in Fig. 1. The torque shown is for only one phase. An average torque will result due to the combined instantaneous values of electromagnetic torque pulses of all machine phases. The machine produces discrete pulses of torque and, by proper design of overlapping inductance profile; it is possible to produce a continuous torque. In actual practice, it will result in reduced power density of the machine and increased complexity of control of the SRM drive.

From Fig. 1, it can be seen that the average torque is controlled by adjusting the magnitude of winding current, I_p or by varying the dwell angle θ_d. To reduce the torque ripples, it is advisable to keep the dwell constant

Corresponding Author: Abdelhamid Boucetta, Faculty of Sciences Engineering, University of Batna,
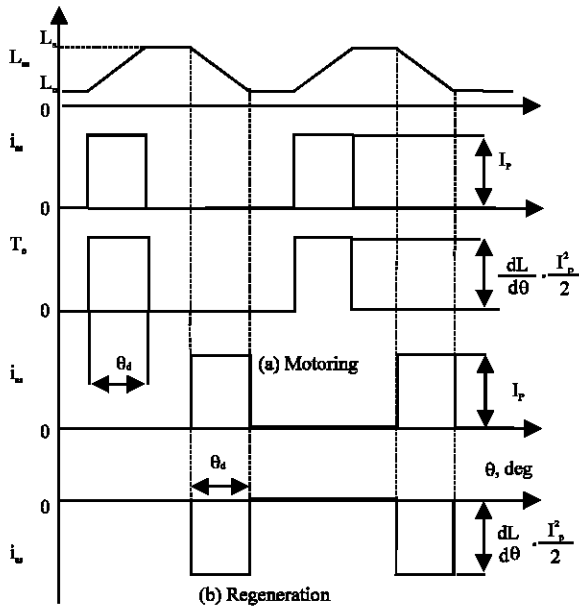Rue Chahid Med Elhadi Boukhlouf, 05000 Batna, Algeria

Fig. 1: Motoring and regeneration action of the SRM

and vary the magnitude of the winding current. The latter approach requires a current controller in the motor drive which incidentally also ensures a safe operation.

MODELING

A general schematic of a drive system (Bae, 2000; Dhulser *et al.*, 2004) shown in Fig. 2 is considered. Practical drive systems may vary from this general schematic. Variations from this block diagram may be minor, are usually confined to the controller section and are specific to applications. Therefore, only common but essential elements of the drive system are given consideration to generalize the procedure. Application-specific controller blocks can be modelled similar to the modelling process developed in the controller subsection. The modelling of various subsystems of the SRM drive is considered in this srtudy. The modelling procedure for the machine in terms of its 3-dimensional relationships of flux linkages, current and rotor positions and air gap torque, current and rotor position is derived. Given a torque command, the current reference for a particular rotor position is found from these three-dimensional relation ships. When the current reference is enforced through a converter, one or more phases of the machine windings are impressed with a voltage. The machine equations, the input voltages and the machine characteristics captured in the 3-dimensional relationships are used to determine the phase currents, air gap torque, rotor speed and rotor position. With the available computed currents and rotor speed, their respective errors are then found for use in the

controller to determine the reference current and torque. This almost completes the tasks of the controller for speed and average torque enforcement. For an instantaneous torque controller, the torque reference to current reference generation is a function of rotor position (Bae, 2000).

Machine modelling: The magnetization characteristics of the machine can be obtained from finite element simulation of the machine given the B-H characteristics of the lamination material, machine dimensions and winding data. Alternatively, they can be computed from the analytical approach (Krishnan, 2001).

However, they may be obtained, a large data set in the form of three-dimensional relationships results for flux linkages vs. current vs. rotor position and air gap torque vs. current vs. rotor position. For currents and rotor positions within the given finite sets there could be infinite sets and for these sets a procedure is required to compute the flux linkages and air gap torque. The handling of such large data sets is a formidable problem in the modeling process.

Some methods are discussed here to model the machine characteristics. Only one phase is considered and its extension to other phases is achieved considering the appropriate position shift between the phases and applying it to the known phase characteristics.

Per phase model: The voltage equation for one phase of the SRM assuming that there is no mutual coupling to other phases is given by:

$$v = R_s i + \frac{d\lambda(\theta,i)}{dt} \tag{1}$$

Where i is the phase current R_s, is the resistance of the phase, v is the voltage applied across the phase winding and $\lambda(\theta, i)$ is the phase flux linkages for a given rotor position θ. and excitation current i. The rate of change of flux linkages with respect to time can be obtained in many ways (Rakgati and Kamper, 2004) assuming that:

$$\lambda(\theta,i) = L(\theta,i).i \tag{2}$$

$$p..\lambda(\theta,i) = L(\theta,i)\Big|_{\theta=const} \frac{di}{dt} + $$

$$+ i \left. \frac{dL(\theta,i)}{dt} \right|_{i=const} \tag{3}$$
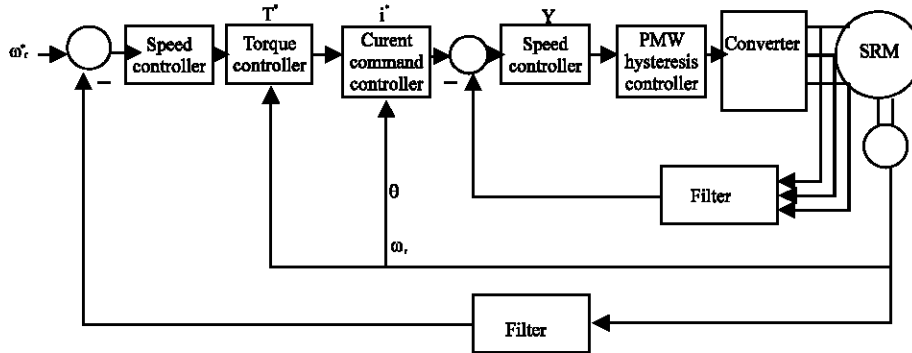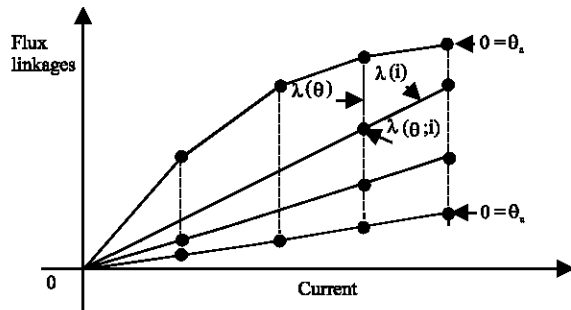
Fig. 2: Closed-loop, speed-controlled SRM drive system

Fig. 3: Phase flux linkages vs. current for varying rotor position

Where p is the derivative operator, d/dt. The inductance L is the self-inductance of the machine phase and it is available as a function of excitation current and rotor position. Also, the derivative of flux linkages can be obtained using partial derivatives as:

$$p.\lambda(\theta,i) = \frac{\partial\lambda(\theta,i)}{\partial i}\frac{di}{dt} + \frac{\partial\lambda(\theta,i)}{\partial\theta}.\frac{d\theta}{dt} \qquad (4)$$

$$p.\lambda(\theta,i) = \ell(\theta,i).\frac{di}{dt} + \omega_m.\frac{\partial\lambda(\theta,i)}{\partial\theta} \qquad (5)$$

Where l (θ, i) is the incremental inductance, so-named because it is the ratio between the incremental flux linkages and incremental excitation current. The incremental inductance is again referred to in on sensorless SRM drives (Milutin *et al.*, 1997). The relationship between the self-inductance and incremental inductance is given by:

$$L(\theta,i) = \frac{1}{i}\int_0^i \ell(\theta,i.)di \qquad (6)$$

The self-inductance is different from the incremental inductance when the operating condition is not linear.

Machine magnetic characteristics representation: Equations 3-5 give different ways of computing the rate of change of flux linkages and are determined by how the machine data can be arranged in a form suitable to realize them through these equations. Whichever may be the equation used in the final solution of the flux linkages and current for a given voltage input, one thing becomes clear upon a cursory glance of the flux linkage equations-it requires a large amount of discrete data. The data are discrete in terms of the current vs. rotor position vs. flux linkages and by using a cubic spline fit, given current and rotor position, the flux linkages can be retrieved. Consider a set of flux linkage vs. phase excitation current vs. rotor position characteristics shown in Fig. 3. The data may have excitation currents of interest (say, from zero to 2 p. u. in usual circumstances and more for specific applications). The rotor position it may cove is from a completely unaligned to fully aligned position given as θ_u and, θ_a, respectively. The retrieval of flux linkages can be achieved in many ways, as discussed in the following. The three-dimensional fit $\lambda(\theta, i)$ of is accomplished by first creating two sets of two-dimensional natural cubic splines. One set contains spline fit curves of $\lambda(\theta)$ for each value of current values and the second set contains the curves of $\lambda(i)$ for each of the rotor positions. The two sets are then described as:

$$\lambda(\theta)\big|_{i\ =i(j)} \quad \text{for } j = 0,1,\ldots\ldots,n_i \qquad (7)$$

$$\lambda(\theta)\big|_{\theta=\theta(k)} \quad \text{for } j = 0,1,\ldots\ldots,n_\theta \qquad (8)$$

Torque representation and its computation: So far, given the discrete data set of flux linkages vs. current vs. rotor

position, the extraction of flux linkages for any current and rotor position has been developed.

The next step in the computation of machine performance is determining the electromagnetic torque that can be obtained from the change in coenergy $\partial W'_f(\theta, i)$, (Luukko, 2000), given as:

$$\partial W'_f(\theta, i) = \int_{i_1}^{i_2} \lambda(\theta, i) \, di \qquad (9)$$

Where the flux linkages are integrated with respect to the phase current for each rotor position. The air gap torque, then, can be calculated for a constant current from the equation as:

$$T_e = \frac{\partial W_f(\theta, i)}{\partial \theta} \qquad (10)$$

The performance computation by algorithm (Huann and Chih, 2004) requires a substantial amount of data and their handling, thus making storage and retrieval time-consuming processes, particularly for online computation and control. A number of efficient methods exist to compute the electromagnetic torque of the system. An adequate method uses spline fit to create 3-dimensional relationships among air gap torque vs. current vs. rotor position. These relationships can then be accessed using the algorithm similar to that developed earlier to retrieve the flux linkages from the stator current and rotor position. Other methods such as neural or fuzzy computation are equally applicable for online retrieval. (Thierry *et al.*, 2007).

Converter: Simulation of the drive system has many objectives, such as validation of the drive system performance, design verification of the machine and design verification of the converter (Thierry, 2003) especially during transients. For drive system performance validation both in steady-state and for dynamic conditions, it can be assumed that the converter is robust between the switching transients, hence the converter power devices can be treated as ideal switches by neglecting the switching transients and voltage drops during conduction. The disadvantage of such an approach is that as the voltage drops across the converter switches an error will be introduced in the switch duty cycle as well as in the power input to the drive system. Their magnitudes will depend on the operational speed of the drive system. At low speeds, the error introduced by the converter switch voltage drop can be significant, while at higher speeds it is negligible. Negligence of the switching transients hardly interferes with the steady

state but can have an impact on the evaluation of switch losses. Therefore, depending on the objective, the converter model can be simple or complex. In the simple model, the power devices can be assumed to be ideal during turnon and turn-off instants and the device voltage drops during conduction are negligible.

Load: A generic load for simulation consists of inertia, friction and load torque, all of which are usually assumed to be constants. The load determines the machine rotor acceleration, speed and position. It is given symbolically as:

$$J.\frac{d\omega_m}{dt} + B.\omega_m = T_e - T_\ell = T_a \qquad (11)$$

Where J is the combined moment of inertia of the motor and load, B is the combined friction coefficient of the motor and load, T_e is the electromagnetic torque, T_l is the load torque T_a and is the acceleration torque. Note that the electromagnetic torque is a function of the rotor position and excitation current. The rotor position is therefore crucial to the control of the machine excitation and is obtained from the speed as:

$$\omega_m = \frac{d\theta}{dt} \qquad (12)$$

In many applications, the inertia and load torques vary during a load cycle and can be functions of rotor position. The load equation has ignored the windage losses, which are proportional to the square of the speed. For speeds higher than 5000 rpm, it is important to incorporate these losses to obtain a realistic load equation, a better estimate of speed and rotor position and a better performance prediction of the SRM. Accurate modelling of the rotor-position-dependent load is essential to study the effect of rotor speed ripples, rotor shaft fatigue and its longevity.

The acceleration torque is periodically triangular with an offset when the generated electromagnetic torque is assumed to be constant. Because of that, the rotor speed is not a smooth ramp during acceleration. When the air gap torque is made to match the load torque but with a dc offset, then the acceleration torque becomes constant, resulting in a smooth ramping of the speed without oscillations.

The discussion so far has pertained to a dynamic situation. During steady state, the rotor speed will have a cyclic variation when the air gap torque is not modified to match the load torque. These cyclic variations of the acceleration torque during steady-

state and dynamic conditions lead to increased audible noise and shaft fatigue (Hofmann and Sanders, 2000).

Controller: The control of an SRM requires an inner current control loop and an outer speed feedback control loop, which is commonly encountered in ac and dc drives. The manner in which the torque and current commands are generated is different in tune with the peculiarities of this machine. The considered controller is capable of giving fine torque control in regard to its ripple content and therefore may be considered to correspond to a high-performance drive system control. Simple applications may not require controllers with torque and current shaping, so the torque command and current command controller blocks can be removed. The simulation of various controllers, such as speed, torque command, current command, current, Pulsed Width Modulation (PWM) and hysteresis current. The relevant equations are derived from the outer to inner loops of the drive system and the reverse is also feasible.

The controller considered in this study is capable of giving fine torque control in regard to its ripple content and therefore may be considered to correspond to a high-performance drive system control. Simple applications may not require controllers with torque and current shaping, so the torque command and current command controller blocks can be removed. The simulation of various controllers, such as speed, torque command, current command, current, Pulsed Width Modulation (PWM) and hysteresis current. The relevant equations are derived from the outer to inner loops of the drive system and the reverse is also feasible.

Speed controller: It is assumed that the speed signal is available and is processed through a filter. The speed signal may be measured directly or obtained from measured rotor position pulses or extracted from estimated rotor position. By whichever manner it is obtained, a number of factors surrounding its acquisition have to be captured in the simulation to reflect the reality: Time delay, attenuation or gain, error characteristics if they are obtained through estimation and linearity, if it is measured, as the error characteristics can handle this aspect in the estimated speed signal case.

The speed controller's input is the speed error that is the difference between the speed reference and the filtered speed feedback signals and its output is the unmodified torque command. In order for the integral part of the speed controller not to be deeply saturated and to provide a responsive operation, an anti-windup controller usually is built into the speed controller in the integral controller path. Individual block diagrams for the speed

filter and the speed controller, including the anti-windup controller, are given in the following discussion and differential, algebraic and conditional relationships are derived from them for inclusion in the simulation.

Torque controller: In low-performance controllers, there is no special torque controller. In that case, the output of the speed controller can be treated as the torque command signal. The disadvantage of such an approach is that the torque command is not conditioned to the peculiarities of the load, such as the cyclic load and the transient and steady-state limits are not embedded in the torque command signal. The former disadvantage has the deleterious effects of speed oscillations and reduced shaft life, whereas the latter can compromise reliable operation. Therefore, it is prudent to modify the torque command with a torque controller in a high performance drive system. Then the factors that may influence the torque controller design are:

* Continuous and intermittent operational limits.
* Load peculiarities, such as continuously varying cyclic loads.
* Individual phase torque command generation primarily to mitigate or eliminate the torque ripple by coordination of individual phase current.

The third factor merits further attention here. Torque ripple reduction is absolutely necessary in SRM drives if they are to find applications in high-performance environments. The reduction is achieved in many ways but most of them are based on the premise that the sum of the air gap torques produced by the outgoing phase and the incoming phase has to be equal to the overall torque command. Therefore, the individual phase torque commands for the outgoing and incoming phases have to be identified for each operating point that is a function of the rotor position. In this method, the slope of the outgoing current is controlled and the radial force can be controlled to mitigate the acoustic noise. A number of advantages can accrue with thistorque command modification in the torque controller. Hereafter, the output of the torque controller will be labeled as a modified torque command. The modelling of this block is then based on the 3 factors discussed. The first 2 factors are easy to incorporate: The first factor as a torque limiter with time constraints and the second factor in the load torque as a function of rotor position and/or speed.

Current command controller: The current controller takes the modified phase torque commands and generates

the phase current commands as a function of rotor position. This is achieved using the three-dimensional torque vs. current magnitude vs. rotor position characteristics of the machine stored in tables and recovered using the algorithm developed earlier. The modeling of the current command controller is likewise accomplished by use of tables containing the machine characteristics (Luukko, 2000).

In low-performance systems, the torque controller is usually absent. In this case, the current command is generated in a slightly different way. The magnitude of the current command is generated from the predetermined steady-state characteristics of the machine. Then, positioning of this stator phase current command with respect to the rotor pole is very crucial. Realizing that the current command needs to be initiated well in advance of the overlap instant of the stator and rotor poles to gain higher speed operation and the current command must be forced to zero well ahead of complete alignment of the poles to minimize or eliminate generation of air gap torque counter to the request, determination of the advance and fall angles is critical to operation of the machine. The inputs to the current controller then consist of torque magnitude, absolute rotor position and advance and fall angles of the phase current. The reference for advance angle is the angle at which the leading rotor pole tip just comes into alignment with the lagging stator pole tip. The fall angle reference is when the stator and rotor poles align. The advance and fall angles usually are predetermined by simulation and programmed into the controller as a function of speed.

The advance and fall angles can be controlled in such a way that the input power is minimized by measuring the input power and incrementally adjusting the angles to determine the local minimum. The search for the minimum input power operating point can be vastly improved by fuzzy control.

Current controller: Current control is achieved with closed-loop control with either a PWM or hysteresis switching control of the converter. The current controller structure is different depending on the switching strategy chosen. The PWM- and hysteresis-based current controllers are therefore discussed separately (Milutin *et al.*, 1997).

PWM current controller: The PWM current controller consists of the following control blocks: Current error generator, a PI current controller, sample-and-hold block and a PWM controller. The PWM controller takes the output of the sample-and-hold circuit and computes the duty cycle and therefore the on and off times in a PWM period for implementation. In hardware implementation,

the on- and off-time gating pulses are generated by comparing the output of the sample-and-hold circuit with a triangular carrier signal. From a modelling point of view, it is easier to consider the analytical computation of the duty cycle and use that information in the generation of gating pulses and applied voltage to the phase windings.

Hysteresis current controller: In the hysteresis switching-based current controller, the current control is much simpler. The current error is computed from which the switching is generated depending on its relationship to the hysteresis current window. Even here, the phase winding energization corresponding to on time, demagnetizing of the winding corresponding to off time and freewheeling corresponding to the interim off times. Discrimination between the freewheeling and demagnetization instances has to be built into the modeling and simulation.

RESULTS AND DISCUSSION

By combining various blocks of the drive system described, system equations are assembled which contain differential, algebraic and conditional equations. The differential equations are solved for a given instant of time starting from zero with small time intervals for integration using one o f the standard techniques such as the Runge-Kutta fourth-order integration method. For faster computation of the system solution, the simpler Euler integration method may be resorted to. It is assumed that the variables are constant over the integration interval and then with the updated values. The algebraic and conditional equations are embedded in the system solution. Because of the large amount of data handling in the system, the task of simulation may initially be daunting. Proceeding systematically and assembling the system equations with the help of a flow chart will make the code assembly a fairly straightforward chore. Some sample results of the simulation are considered.

A more demanding application of this technique is in load compensation and is demonstrated here with a compressor load. Without and with load compensation dynamic simulation results are shown in Fig. 4a and b, respectively. Consider that the electromagnetic torque of the motor is constant, resulting in a varying acceleration torque, which, in turn, produces an oscillatory speed response for an inertial load as shown in Fig. 4a. Such oscillatory speed behavior fatigues the shaft, increases its wear and tear and results in audible noise generation. These effects reduce the life of the compressor and cause discomfort to the users. They could be overcome if the electromagnetic torque is made to match the load torque and to generate the required acceleration torque uniformly
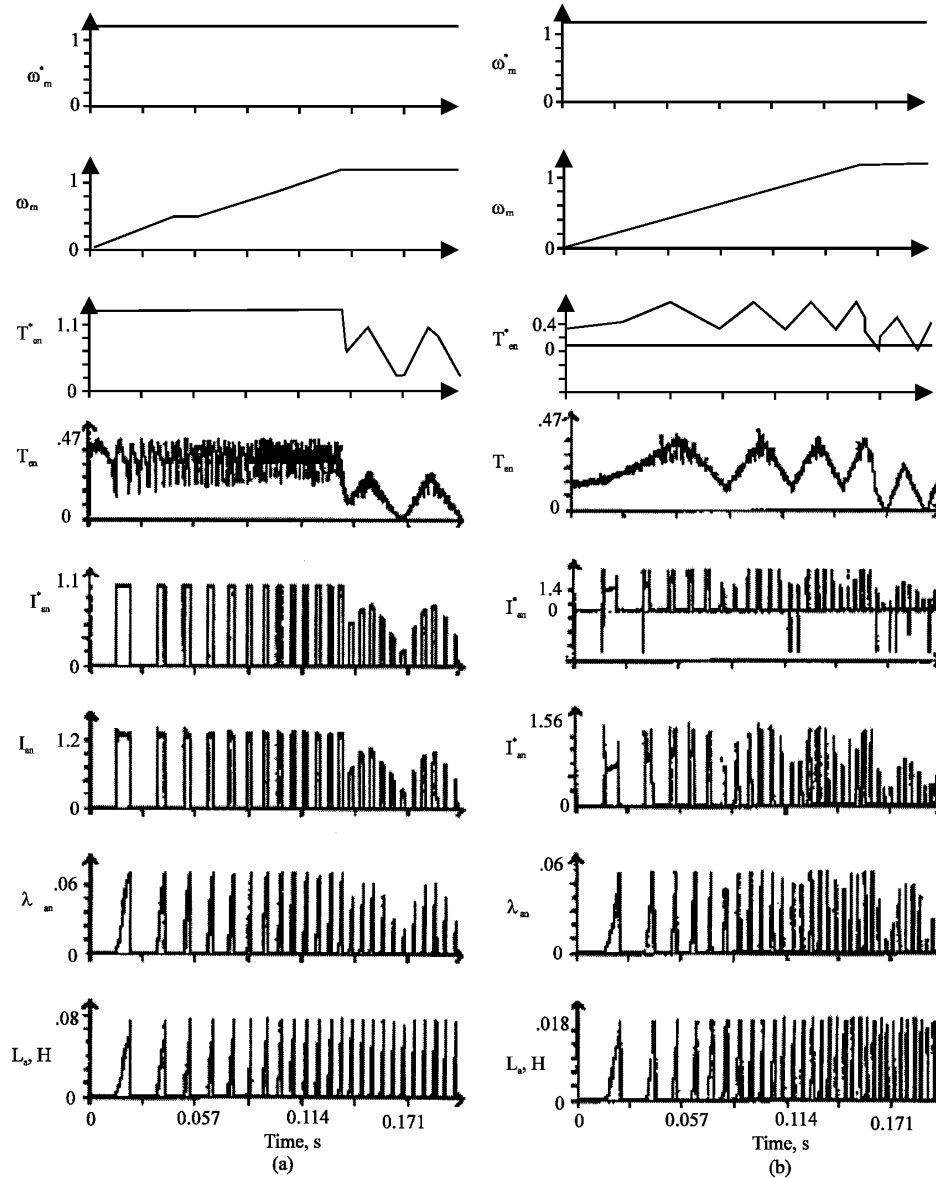
Fig. 4: a) Performance of the speed controlled drive with speed matching, b) Performance of the speed drive without load matching

as shown in Fig. 4b, resulting in a smooth speed response. Note that compensation by modifying the electromagnetic torque is achieved to match the load torque during both steady and transient states. The speed oscillations are eliminated with load compensation, as can be seen from the simulation results.

As a result, it is shown that varying acceleration torque, which leads in audible noise generation, could be overcome if the electromagnetic torque is matched with the load torque generating a uniformly the required acceleration torque; in turn, resulting in a smooth speed response. Also, the speed oscillations are eliminated with load compensation.

CONCLUSION

Modelling and simulation of the SRM Drive System is presented in this study, where the torque production factors are considered. Modelling of different subsystems is realised in order to study the SRM drive performance.

REFERENCES

Bae, H.K., 2000. Control of switched reluctance motors considering mutual inductance, Ph.D. Thesis, The Bradley Department of Electrical and Computer Engineering, Virginia Technol., Blacksburg, VA.

D'hulster, F., K. Stockman and R.J.M. Belmans, 2004. Modelling of switched reluctance machines: State of the art, IASTED., 24: 216-224.

Hofmann, H. and S.R. Sanders, 2000. High-Speed synchronous reluctance machine with minimized rotor loss, IEEE. Trans. Industry Applications, 36: 531-539.

http://www.mathworks.com/access/helpdesk/help/toolbox/physmod/powersys/powersys.html.

Huann-Keng Chianga and Chih-Huang Tsen, 2004. Design and implementation of a grey sliding mode controller for synchronous reluctance motor drive, Science Direct ,Control Eng. Practice, 12: 155-163.

Krishnan, R., 2001. Electric Motor Drives: Modelling, Analysis and Control, Prentice-Hall, NJ.

Luukko, J., 2000. Direct torque control of permanent magnet synchronous machine-Analysis and Implantation, Doctorate Thesis, Helsinki, University of Technology, FINLAND.

Milutin, G. Jovanovit and Robert E. Betzt, 1997. Maximum Torque Control of a Sensorless Synchronous Reluctance Motor Drive, IEEE Industry Applications Society Annual Meeting New Orleans, Louisiana, pp: 5-9.

Rakgati, E.T. and M.J. Kamper, 2004. Torque Performance of Optimally Designed Three and Five phase Synchronous Reluctance Machines with Two Rotor Structures, IEEE. AFRICON., 1: 625-630.

Thierry Lubin , Hubert Razik and Abderrezak Rezzoug, 2007. On-line efficiency optimization of a synchronous reluctance motor, Science Direct, Electric Power Sys. Res., 77: 484-493.

Thierry LUBIN, 2003. Modélisation et commande de la machine à reluctance variable: Prise en compte la saturation magnétique, Doctorate Thesis, France, Univercity of Henri Poincaré, NANCY-1, FRANCE.